Numerical Investigation of the Influence of Aerodynamic Forces and Wheel Dynamic Loads of a Vehicle Subjected to Kinematic Excitations

Michał MAKOWSKI
Warsaw University of Technology, Institute of Vehicles,
ul. Narbutta 84, 02-524 Warszawa, michal.makowski1@pw.edu.pl

Wiesław GRZESIKIEWICZ
Warsaw University of Technology, Institute of Vehicles,
ul. Narbutta 84, 02-524 Warszawa, wgr@simr.pw.edu.pl

Abstract

This paper presents the investigations of vibrations of a vehicle equipped with controlled magneto-rheological (MR) dampers and aerodynamic elements. A scaled sports vehicle model was developed to conduct this research. The tests were carried out with kinematic excitation resulting from road roughness and motion at a variable speed. During the airflow, the aerodynamic elements forces and moments on the test body. Vehicle vibrations are limited by the means of MR controlled dampers. The damping force is determined on the basis of an algorithm, where various strategies for determining forces in MR damper have been adopted. Two criteria were considered for assessing the effectiveness of the control algorithm - minimising vertical acceleration and changes in wheel normal reactions on road surface. This paper presents the results of those studies.

Keywords: magneto-rheological damper, vehicle, control algorithm, vibration

1. Introduction

This paper addresses vibrations of a vehicle moving at high speed during acceleration or deceleration. The system vibrations are determined with the application of a model as stipulated in the papers [2, 6] presenting a mathematical model of a vehicle being equipped with magneto-rheological (MR) [6, 10] or with other controlled dampers described in [3, 4, 9]. It causes an occurrence of the inertia force being a reason for a change of wheels normal reaction forces on a road surface leading towards the wheel slip. In order to avoid this problem, high-speed vehicles are equipped with special aerofoils to generate higher normal reactions on road [7, 11].

The main objective of the work is to propose the methodology to take into account the impact of vehicle longitudinal acceleration and aerodynamic forces and qualitative and quantitative assessment of this influence on the level of wheel dynamic loads. The authors investigated the vibrations caused by unevenness of the road surface, inertia forces acting on the vehicle's body when accelerating and decelerating, as well as aerodynamic forces. The paper presents simulated tests conducted using the model described in [5]. The discussed model has been upgraded with an influence of the aerodynamic forces on the vehicle's vibration.

2. Aerodynamic forces and moments

In [1, 5, 11] an extensive analysis is presented on the influence of air flow on the moving vehicle. The resultant influence of air pressure on the vehicle's surface is determined by three forces and moments – presented in Figure 1 in the vehicle's local coordinate system.

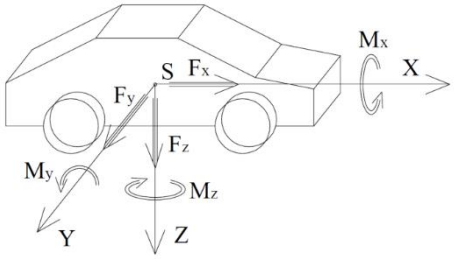

Figure 1. Problem schematic and its coordinate system

Due to the distribution complexity of the air pressure on the vehicle's surface, the effect was assumed to act in a steady motion, utilising the resultant force and moment. The description of these forces and moments, following the convention from Figure 1, is usually presented in the following form:

$$F_x = \frac{1}{2}\rho V^2 A c_x,\ \ F_y = \frac{1}{2}\rho V^2 A c_y,\ \ F_z = \frac{1}{2}\rho V^2 A c_z$$
$$M_x = \frac{1}{2}\rho V^2 A l c_{mx},\ \ M_y = \frac{1}{2}\rho V^2 A l c_{my}, \tag{1}$$
$$M_z = \frac{1}{2}\rho V^2 A l c_{mz}$$

where: ρ – air density, V – vehicle velocity, A – frontal area of the vehicle, l – vehicle wheelbase, c_x, c_y, c_z – dimensionless coefficients of aerodynamic forces: frontal, side, down force (or lift), c_{mx}, c_{my}, c_{mz} – dimensionless coefficients of aerodynamic moments of forces: tilting, inclining, deflecting.

The values of those aerodynamic coefficients are determined based on the measurement results obtained in wind tunnels [1, 7, 11].

As this consideration is limited to vertical vibrations in a rectilinear motion, only F_z force and M_y moment will be considered and the rest of the aerodynamic forces will be neglected. For convenience, some other equivalent dimensionless aerodynamic coefficients determining pressure on the front and rear axles will be considered.

$$c_1 := \frac{a_2}{l} c_z - c_{my},\ \ c_2 := \frac{a_1}{l} c_z - c_{my} \tag{2}$$

where: a_1, a_2 – dimensions marked in the Figure 2.

Aerodynamic forces pressing the axles down are computed as per the following formula:

$$N_1 = \frac{1}{2}\rho V^2 A c_1,\ \ \ N_2 = \frac{1}{2}\rho V^2 A c_2 \tag{3}$$

It should be noted that all of the aforementioned aerodynamic forces act on the vehicle's body. Moreover, one must realize that F_z force refers to the downforce pressing the vehicle's body to the road while in common practice the considerations are based on lift, conventionally facing in the opposite direction.

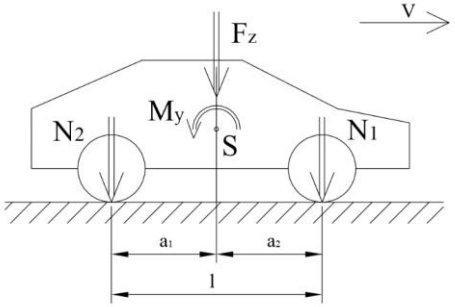

Figure 2. Scheme of vehicle's body aerodynamic forces, Fz – resultant downforce, My –inclining moment, N_1 – downforce of the front axle, N_2 – downforce of the rear axle

In some high-speed cars, one might find controllable aerodynamic wings being able to adjust its position to maximize the aerodynamic forces depending on conditions. Within this work an additional tilting moment ΔM_y resulting from the aerofoil geometry is included in the considerations.

$$\Delta M_y = \frac{1}{2}\rho V^2 A l \Delta c_{my} \tag{4}$$

Where in variable Δc_{my} is given by the formula:

$$\Delta c_{my} \epsilon [-\Delta c_{my0}, +\Delta c_{my0}] \tag{5}$$

where Δc_{my0} indicates a limit value of coefficient Δc_{my}.

The value of Δc_{my} coefficient characterizes the aerodynamic configuration of the aerofoil. In this paper, it will be adjusted to the vehicle's longitudinal acceleration in order to decrease the axle load caused by the inertial force of the body.

The moment of force induced by the controlled aerofoil can also be expressed by a change of the normal reactions on road.

$$\Delta N_1 = -\frac{\Delta M_y}{l}, \quad \Delta N_2 = +\frac{\Delta M_y}{l} \tag{6}$$

3. Description of the vehicle's model

A detailed description of the vehicle's mathematical model is provided in [5] and [10]. The model was adopted in a form of a mechanical system, as presented in Figure 2 along with the coordinates describing the respective wheels degrees of freedom.

The model under consideration describes the vehicle equipped with magneto-rheological (MR) dampers, controlled in order to decrease the total level of vibration. Attenuating forces in MR dampers were assumed to act to minimize the square of norm of the body acceleration vector. Leading the following expression to reach the minimum at any time, where w_x, w_y [m^2] – weighting coefficients.

$$\mathcal{K} := \ddot{z}^2 + w_x\left(\ddot{\Phi}_x\right)^2 + w_y\left(\ddot{\Phi}_y\right)^2 \left[\frac{\mathrm{m}^2}{\mathrm{s}^4}\right] \tag{7}$$

The vehicle's parameters assumed for simulation purposes are presented below. It should be noted that vehicle model discussed within [5, 6] was upgraded with the aerodynamic forces $F_z, M_y, \Delta M_y$ according to the relations given above in formulas (1), (4), (5) and (6).

The following parameters defining the vehicle were adopted: $m = 1250$ kg – mass of the vehicle's body; $m_0 = 25$ kg – reduced mass of the wheel and components of suspension; $J_x = m\rho_x,\ \rho_x = 0.6$ m – moment of inertia of the body relative to the longitudinal axis; $J_y = m\rho_y,\ \rho_y = 1.15$ m – moment of inertia of the body relative to the transverse axis; $a_1 = 1.4$ m, $a_2 = 1.45$ m, $b_1 = b_2 = 0.725$ m – dimensions determining the position of the centre of the body's mass relative to the wheels, where b_1, b_2 - represent the track width of the front and rear axles of the vehicle.; $k_1 = k_2 = 14.5$ kN/m – stiffness of the front and rear wheels'suspension; $k_0 = 200$ kN/m – stiffness of the wheel tire; $c_0 = 2.5 \cdot 10^5$ Ns/m – tire damping coefficient.

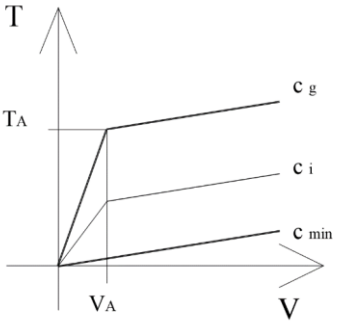

Figure 3. Assumed characteristics of MR damper

The characteristics of magneto-rheological dampers are depicted in Figure 3. The following parameters were assumed: $T_A = 400$ N, $V_A = 0.0075$ m/s, $c_{min} = 210$ Ns/m, $I_{max} = 2$A (Fig. 3). All of the other parameters regarding the electric power supply system were adopted as per [8, 12].

Moreover, the authors assumed the vehicle to move on a road with an irregularity described by the following function: $\xi(s) = \xi_0 \sin 2\pi \frac{S}{L}$, where $\xi_0 = 5$ mm, $L = 12$ m, s – travelled distance, additionally, the surface profiles were assumed to be shifted in phase by $\Delta s = a_1$. The vehicle moves with a time-dependent speed as presented in Figure 4. The vehicle moves at variable speed to obtain different aerodynamic forces on the flaps. Initially, the vehicle accelerates is $\ddot{x} = 2.85$ m/s^2 and then drives at constant speed of

100 km/h . After 15 seconds the vehicle accelerations to 150 km/h and in the last distance it moves with constant speed 50 km/h.

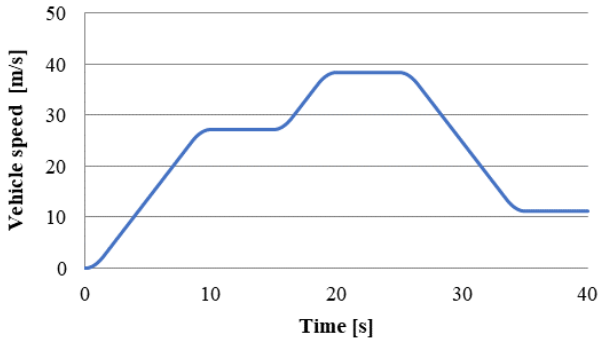

Figure 4. The vehicle speed versus time

Since the investigation conducted had only a comparative purpose, the reference vehicle was assumed to be equipped with the standard dampers characterized by two coefficient: $c_1 = 500$ Ns/m – when damper is compressed, $c_2 = 2.5 \cdot c_1$ – when damper is extended.

To compute the aerodynamic forces, the following data was adopted $\rho = 1.225$ kg/m^3 – air density, $A = 1.74$ m^2 – cross-sectional area of the vehicle, $c_z = 0.2$, $c_{my} = 0.04$ – nominal values of aerodynamic drag coefficients. The Δc_{my0} coefficient is changed when the acceleration of the vehicle is greater than $+/-1$ m/s^2. When the vehicle accelerates, we take the value $\Delta c_{my0} = -0.1$, it causes the front axle to be overloaded. In case of braking, the value $\Delta c_{my0} = 0.1$, and this causes the rear axle to be overloaded.

4. Results of simulations

Simulations were performed with the speed given by the relationship depicted in Figure 4. Changing the acceleration of the vehicle causes the inertial forces that cause body roll. These forces can be reduced by external forces, which are formed on the aerodynamic elements. Additionally, the vibration of a vehicle were excited from the ground by the function in the form of $\xi(s)$. These vibrations can be reduced by using MR dampers.

In order to rate intensity of the vehicle body vibration two indicators were proposed. First one defined as a sum of squares of acceleration at points of the body located above the wheels of the vehicle.

$$W_P := \left(\int_0^{t_{\text{end}}} \sum_{i=1}^{4} P_i^{\,2}(t)\,\mathrm{d}t \right)^{1/2}, \quad t_{\text{end}} = 40 \text{ s} \tag{8}$$

where: P_i, $i = 1, \ldots, 4$ – functions defining accelerations at the specified points of vehicle body.

The second indicator is based on variation of wheels normal reaction relative to the static normal force.

$$W_N := \left(\int_0^{t_{\text{end}}} \sum_{i=1}^{4} F_i^{\,2}(t)\,\mathrm{d}t \right)^{1/2}, \quad t_{\text{end}} = 40\ \text{s} \tag{9}$$

where: F_i, $i = 1, \ldots, 4$ – functions describing deviation coefficient of normal reaction (1 – right wheel on front axle, 2 – right wheel on rear axle, 3 – left wheel on front axle, 4 - left wheel on rear axle), given by:

$$F_i = \frac{\Delta N_i}{Q_i} \tag{10}$$

where: ΔN_i – deviation of normal reaction during vehicle vibration, Q_i – wheel static load equals for the wheels.

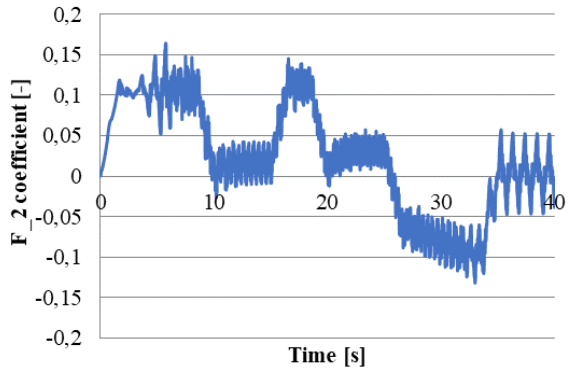

Figure 5. Influence of the aerodynamic forces on a deviation of normal reaction on the road surface – case I (MR damper) – rear axle

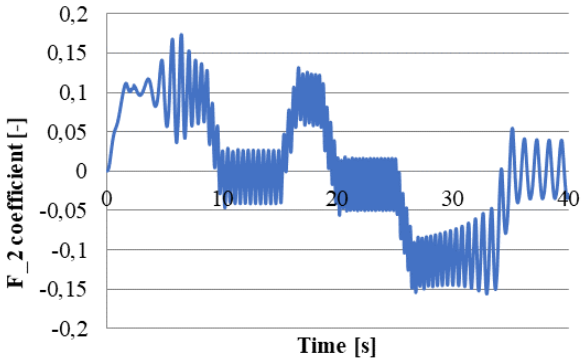

Figure 6. Influence of the aerodynamic forces on a deviation of normal reaction on the road surface – case II (classical damper) – rear axle

The influence of the aerodynamic forces on the deviation of normal reaction on the road surface was presented with the application of relative force plots. This might be defined as a ratio of a deviation and static value of normal reaction of the rear axle. The presented simulation results have only exemplary meaning. Figure 5 presents the results for case I (tab. 1) of the vehicle with MR dampers and Figure 6 presents the results for case II (tab. 1) of the vehicle with classical dampers.

Table 1. Values of coefficient c_z and type of damper for different cases

Case	Coefficient c_z	Damper
I	-0.2	MR
II	0.2	Classical

The comparative analysis of the influence of aerodynamic forces was carried out considering only negative values from the figures, determining the axle underload relative to the static load.

Table 2. Values of coefficients W_P and W_N

Case	W_P	W_N
I	3.095	0.448
II	4.958	0.494

Comparing the graphs (Fig. 5 and Fig. 6) for case I and II, it can be stated that the application of MR dampers results in a decrease of the axle load oscillation amplitude of the factor F_2. This led to a decrease of the axle load instantaneous values during vehicle braking, observable in the range [27 s ÷ 34 s]. The average value was determined in this range on the basis of the trend line. This value was - 0.08 in the case of I (Fig. 5), and in the case of II (Fig. 6) it was - 0.11. This change is related to the action of aerodynamic forces. In the discussed section, there is also a visible decrease in the values of amplitudes, where in the case of I the value of the amplitude is about 0.03 and in the case of II it is about 0.05. The reduction of the changes of the amplitudes of the rear axle wheel normal reaction forces on the road surfaces ΔN_2 is associated with the control of the MR damper.

Table 2 presents the comparison of the accelerations factor and the dynamic load factor. In case I of using MR controlled dampers and control of the aerodynamic flap, the acceleration ratio was reduced (37.5%) and the dynamic load factor was kept constant compared to vehicle with classic suspension.

5. Summary

This paper considered the influence of aerodynamic forces on a vehicle's vibration during its rectilinear motion with a variable velocity. In order to assess this, two indicators determining the intensity of body vibration and also changes in wheels normal reactions on road on a road surface were chosen.

The values of the chosen indicators were determined based on the simulation results of vehicle vibration during a 40-second run with variable velocity.

Based on the comparative analysis of the test results depicted in table 1 and the graphs illustrating the axels normal reactions on road surface it might be stated that: the utilisation of MR dampers significantly reduced the vehicle's body accelerations and fluctuations in wheel normal reactions on road.

The results of the investigations showed that the use of controlled MR dampers and controlled flap reduced the acceleration factor as well as kept the dynamic load factor constant compared to the results of vehicle tests with classic dampers.

Acknowledgments

This project was funded by the Polish National Centre for Research and Development allocated on the basis of the decision number PBS3/B6/34/2015.

References

1. R. Bansal, R. B. Sharma, *Drag reduction of passenger car using add-on devices*, Journal of Aerodynamics, Volume 2014, Article ID 678518, 13 pages.
2. M. W. Dobry, *Energy Analysis of a Mechanical System with a Dynamic Vibration Absorber*, Vibrations in Physical Systems, **27** (2016) 10-1 – 10-8.
3. R. Faraj, C. Graczykowski, *Hybrid Prediction Control for self-adaptive fluid-based shock-absorbers*, Journal of Sound and Vibration, **449** (2019) 427 – 446, DOI: 10.1016/j.jsv.2019.02.022.
4. C. Graczykowski, R. Faraj, *Development of control systems for fluid-based adaptive impact absorbers*, Mechanical Systems and Signal Processing, ISSN: 0888-3270, DOI: 10.1016/j.ymssp.2018.12.006, **122** (2019) 622 – 641.
5. W. Grzesikiewicz, M. Makowski, *Optimisation of vehicle vibration damping in a semi-active system*, Modelowanie Inżynierskie, **68** (2018) 38 – 46.
6. D. C. Karnopp, *Active damping in road vehicle suspension system*, Vehicle System Dynamics, **12** (1983) 183 – 188.
7. K. Kurec, M. Remer, J. Broniszewski, M. Bibik, S. Tudruj, J. Piechna, *Research Article Advanced Modeling and Simulation of Vehicle Active Aerodynamic Safety*, Journal of Advanced Transportation, Volume 2019, doi.org/10.1155/2019/7308590, 2019.
8. M. Makowski, L. Knap, *Investigation of an off-road vehicle equipped with magnetorheological dampers*, Advances in Mechanical Engineering, **10**(5) (2018) 1 – 11, DOI: 10.1177/1687814018778222.
9. M. Michajłow, T. Szolc, Ł. Jankowski, R. Konowrocki, *Semi-Active Reduction of Vibrations of Periodically Oscillating System*, Solid State Phenomena, **248** (2016) 111 – 118, DOI 10.4028/www.scientific.net/SSP.248.111.
10. M. Rosłół, B. Sapiński, *Ability Of Energy Harvesting Mr Damper To Act As A Velocity Sensor In Vibration Control Systems*, Acta Mechanica Et Automatica, **13**(2) (2019) DOI 10.2478/ama-2019-0019.
11. T. Schütz, *Hucho-Aerodynamik des Automobils*, Springer Fachmedien Wiesbaden, 2013.
12. Thomas Lord Research Center, *www.mrfluid.com*, 2019.